The Extended Milling Bifurcation Diagram

Tony L. Schmitz and Andrew Honeycutt
University of North Carolina at Charlotte, Charlotte, NC
tony.schmitz@uncc.edu

Abstract
This paper describes the extended milling bifurcation diagram which can be used to gain fundamental new insights into milling dynamics. The diagram is constructed using numerical simulation techniques and provides both stability behavior (such as Hopf and period-*n* bifurcations) and vibration amplitudes under stable and unstable conditions. The results are compared to semi-analytical stability predictions. It is expected that the insights gained through the extended milling bifurcation diagram will reveal new milling strategies that yield increased productivity and reduced costs for subtractive, discrete part manufacturing.

Keywords: Machine tool, milling, dynamics, stability, bifurcation

1 Introduction

In science and engineering fields, new discoveries are typically followed by a burst of follow-on research activity and corresponding publications. These discoveries tend to serve as a catalyst to the research community and often result in new insights, improved understanding of fundamental phenomena, and enhanced modeling capabilities. For machining, one such period of rapid progress began in the mid-19th century (Arnold). During this time, self-excited vibrations were first described using time-delay differential equations (Doi and Kato). The notion of "regeneration of waviness" was promoted as the feedback mechanism (time-delay term), where the previously cut surface combined with the instantaneous vibration state dictates the current chip thickness, force level, and corresponding vibration response (Tobias and Fishwick, Tlusty and Polacek, Tobias, Merritt). This work resulted in analytical algorithms that were used to produce the now well-known stability lobe diagram that separates the spindle speed-chip width domain into regions of stable and unstable behavior (Tobias, Merritt, Tlusty and Polacek, Shridar *et al.* 1968a, Hohn *et al*., Shridar *et al*. 1968b, Hanna and Tobias, Tlusty and Ismail 1981, Tlusty and Ismail 1983, Tlusty 1985, Tlusty 1986, Minis and Yanusevsky, Altintas and Budak); see Fig. 1.

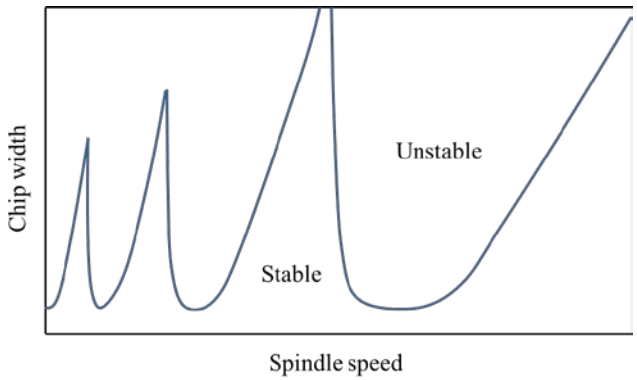

Figure 1. Example stability lobe diagram.

In 1998, a similar step forward in the understanding of machining behavior was realized. Davies *et al*. used once-per-revolution sampling to characterize the synchronicity of cutting tool motions (measured using a pair of orthogonal capacitance probes) with the tool rotation in milling (Davies *et al*. 1998). This approach was an experimental modification of the Poincaré maps used to study state space orbits in nonlinear dynamics. They observed the traditional quasi-periodic chatter associated with the secondary (subcritical) Hopf, or Neimark-Sacker, bifurcation* that can occur for systems described by periodic time-delay differential equations (Moon and Kalmár-Nagy). This was an expected result and was observed as an elliptical cluster of once-per-revolution sampled points in the *x-y* measurement plane perpendicular to the endmill axis as depicted in Fig. 2a. This elliptical collection of points occurred because the chatter frequency was incommensurate† with the tooth passing frequency and quasi-periodic behavior was obtained. However, they also recorded period-3 tool motion (i.e., motion that repeated with a period of three cutter revolutions) during partial radial immersion milling. This period-3 motion manifested itself as three distinct clusters of once-per-revolution sampled points in the *x-y* plane; see Fig. 2b. They noted that this behavior was "inconsistent with existing theory" (Davies *et al*. 1998).

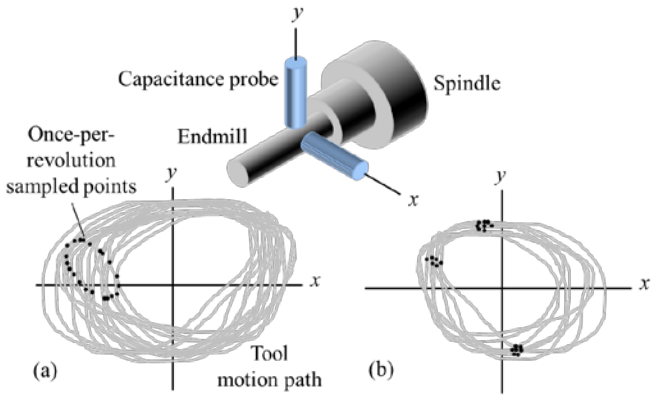

Figure 2. Once-per-revolution sampling of cutting tool motions (a) Hopf instability; (b) period-3 instability.

* A bifurcation is a dramatic change in the system state, or behavior.
† Two values are incommensurate if their ratio cannot be expressed as a ratio of whole numbers.

In 2000, Davies *et al.* further examined the stability of highly interrupted (or low radial immersion) milling (Davies *et al*. 2000). They developed a two-stage map to describe:

1. non-cutting motions governed by an analytical solution (damped free vibration); and
2. motions during cutting using an approximation (fixed tool position with a change in momentum).

They reported a doubling of the number of optimally stable spindle speeds when the time in cut is small (i.e., low radial depth of cut). These extra spindle speeds, Ω (rpm), were defined using the (dominant) damped natural frequency, f_d (Hz), of the structural dynamics, and number of cutter teeth, N_t:

$$\Omega = \frac{2 f_d}{N_t j} \cdot 60 \tag{1}$$

where j = 1, 3, 5, … The traditional secondary Hopf bifurcation lobes correspond to j = 2, 4, 6, … Milling experiments confirmed the new, low radial immersion best speeds.

In 2001, Moon and Kalmár-Nagy reviewed the "prediction of complex, unsteady and chaotic dynamics" in machining (Moon and Kalmár-Nagy). They listed the various contributors to nonlinear behavior, including the loss of tool-workpiece contact due to large amplitude vibration and workpiece material constitutive relations, and highlighted previous applications of nonlinear dynamics methods to the study of chatter (Moon, Bukkapatnam *et al.*, Stépán and Kalmár-Nagy, Nayfey *et al*., Minis and Berger, Moon and Johnson). They also specified the use of phase-space methods, such as Poincaré maps, to identify changes in machining process dynamics.

Time-domain simulation offers a powerful tool for exploring milling behavior and has been applied to identify instability (Smith and Tlusty, Campomanes and Altintas). For example, Zhao and Balachandran implemented a time-domain simulation which incorporated loss of tool-workpiece contact and regeneration to study milling (Zhao and Balachandran). They identified secondary Hopf bifurcation and suggested that "period-doubling bifurcations are believed to occur" for low radial immersions (Zhao and Balachandran). They included bifurcation diagrams for limited axial depth of cut ranges at two spindle speeds to demonstrate the two bifurcation types.

Davies *et al.* extended their initial work in 2002 to present the first analytical stability boundary for highly interrupted machining (Davies *et al*. 2002). It was based on modeling the cutting process as a kicked harmonic oscillator with a time delay and followed the two-stage map concept described previously (Davies *et al*. 2000). They used the frequency content of a microphone signal to establish the existence of both secondary Hopf and period-2 (period-doubling or flip) instabilities. Mann *et al*. also provided experimental validation of secondary Hopf and period-2 instabilities for up and down milling (Mann *et al*. 2003b). They reported "a kind of period triple phenomenon" (Mann *et al*. 2003b) observed using the once-per-revolution sampled displacement signal recorded from a single degree of freedom flexure-based machining platform.

The semi-discretization, time finite element analysis, and multi-frequency methods were also developed to produce milling stability charts that demonstrate both instabilities (Mann *et al*. 2003, Insperger *et al*. 2003, Insperger and Stépán, Mann *et al*. 2004, Merdol and Altintas Y). In (Govekar *et al*.), it was shown using the semi-discretization method that the period-2 bifurcation exhibits closed, lens-like, curves within the secondary Hopf lobes, except for the highest speed stability lobe; see Fig. 3, where b is the axial depth of cut for peripheral milling. Simultaneous quasi-periodic (secondary Hopf) and period-2 bifurcation behavior was also observed. It was reported that this "combination" behavior occurred at unstable axial depths of cut above the period-2 lobes. Additionally, period-3 instability was seen and it was noted that this "periodic chatter" with period-3 (or higher) always occurred above a secondary Hopf stability limit. The same group (Gradišek *et al*.) reported further experimental evidence of quasi-periodic (secondary Hopf), period-2, period-3, period-4, and combined quasi-periodic and

period-2 chatter, depending on the spindle speed-axial depth values for a two degree of freedom dynamic system. A perturbation analysis was performed in (Mann *et al*. 2005) to identify the secondary Hopf and period-2 instabilities. Additionally, numerical integration was implemented to construct a bifurcation diagram for a selected spindle speed that demonstrated the transition from stable operation to quasi-periodic chatter as the axial depth is increased.

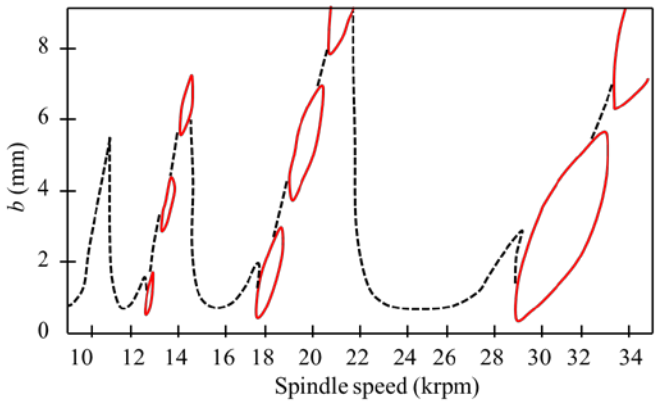

Figure 3. Stability lobe diagram with Hopf (dashed) and period-2 (solid) stability boundaries (Govekar *et al*.).

Stépán *et al*. continued to explore the nonlinear aspects of milling behavior in 2005 (Stépán *et al*.). They described stable period-2 motion where the tool does not contact the workpiece in each tooth period (even in the absence of runout). For a two flute cutter, for example, only one tooth contacts the workpiece per revolution; they referred to this condition as the "fly over effect" and included a bifurcation diagram for these proposed stable and unstable period-2 oscillations.

The effect of the helix angle on period-2 instability was first studied by (Zatarain *et al.*). They found that, depending on the helix angle, the closed, lens-like, curves within the secondary Hopf lobes change their size and shape. They also found that these closed islands of stability can appear even in the highest speed stability lobe (in contrast to the results when helix angle is not considered). Experimental results were provided. This work was continued in (Insperger *et al*. 2006), where the authors emphasized that at axial depths equal to the axial pitch, p, of the cutter teeth:

$$p = \frac{d\pi}{N_t \tan(\gamma)}, \tag{2}$$

the equation of motion becomes an autonomous delay differential equation so the period-2 instability is not possible (d is the cutter diameter, N_t is the number of teeth, and γ is the helix angle). Therefore, axial depths that are integer multiples of p form the horizontal boundaries between the stability islands. Patel *et al*. also studied the helix effect in up and down milling using the time finite element approach (Patel *et al*.).

2 Bifurcation Diagrams

A bifurcation diagram enables the evolution of system behavior (e.g., tool motion) with a control variable of interest (such as axial depth of cut in milling) to be efficiently observed. The diagram uses

the periodic sampling strategy to identify periodic (or aperiodic) responses over the selected range of the control variable. For milling, the tool motion in the feed, *x*, or *y* direction is sampled once per spindle revolution for a given axial depth of cut (and fixed spindle speed). This produces a sequence of points over multiple cutter revolutions (see Fig. 2 for example). This collection of points is then truncated to remove the transient portion of the motion (typically the first few milliseconds).

For stable milling with motion that is periodic with the cutting force (i.e., only forced vibrations are present), these sampled points repeat each revolution because the cutting force and subsequent vibration response is periodic with the spindle rotation. The superposition of all these repeated points therefore gives a single point (or nearly so) on a bifurcation diagram of axial depth (horizontal axis) versus once-per-revolution sampled tool motion (vertical axis).

For a higher axial depth at the same spindle speed, secondary Hopf instability may occur and then the motion is quasi-periodic with tool rotation because the chatter frequency is (generally) incommensurate with the tooth passing frequency. In this case, the once-per-revolution sampled points do not repeat and they form a distribution (as shown in Fig. 2a). When plotted on the bifurcation diagram, this distribution appears as a vertical "spread" of points.

For period-2 instability, on the other hand, the motion repeats only once every other cycle (i.e., it is a sub-harmonic of the forcing frequency). In this case, the once-per-revolution sampled points alternate between two solutions. On the bifurcation diagram, the points appear in two distinct vertical locations (recall that the vertical axis is the sampled tool motion). For period-*n* instability, the sampled points appear at *n* vertical locations. The bifurcation diagram construction from results at multiple axial depths of cut for a selected spindle speed is depicted in Fig. 4.

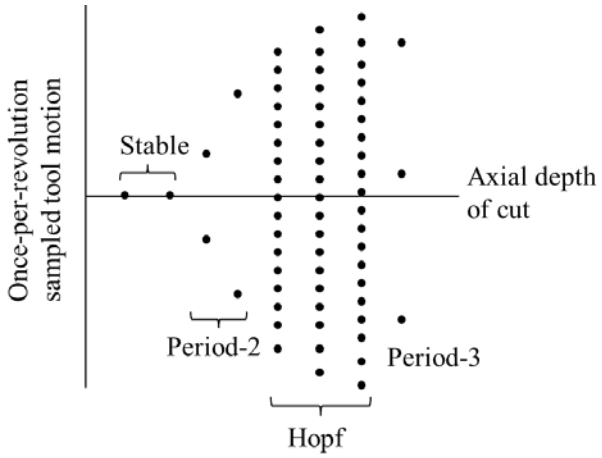

Figure 4. Description of stable/unstable behavior for a milling bifurcation diagram.

3 Time-domain Simulation

Time-domain simulation entails the numerical solution of the governing equations of motion for milling in small time steps. It is well-suited to incorporating all the intricacies of milling dynamics, including the nonlinearity that occurs if the tooth leaves the cut due to large amplitude vibrations and complicated tool geometries (including runout, or different radii, of the cutter teeth, non-proportional teeth spacing, and variable helix). The simulation is based on the *Regenerative Force, Dynamic Deflection Model* described by (Smith and Tlusty). As opposed to stability lobe diagrams that provide a "global" picture of the stability behavior, time-domain simulation provides information regarding the

"local" cutting force and vibration behavior (at the expense of computational efficiency) for the selected cutting conditions. The simulation proceeds as follows:

1. the instantaneous chip thickness is determined using the vibration of the current and previous teeth at the selected tooth angle
2. the cutting force is calculated
3. the force is used to find the new displacements
4. the tooth angle is incremented and the process is repeated. Modal parameters are used to describe the system dynamics in the *x* (feed) and *y* directions, where multiple degrees of freedom in each direction can be accommodated.

The instantaneous chip thickness depends on the nominal, tooth angle-dependent chip thickness, the current vibration in the direction normal to the surface, and the vibration of previous teeth at the same angle. The chip thickness can be expressed using the circular tool path approximation as $h(t) = f_t \sin(\phi) + n(t-\tau) - n(t)$, where f_t is the commanded feed per tooth, ϕ is the tooth angle, n is the normal direction, and τ is the tooth period. The tooth period is defined as $\tau = \frac{60}{\Omega N_t}$ (sec), where Ω is the spindle speed in rpm and N_t is the number of teeth. The vibration in the direction of the surface normal for the current tooth depends on the *x* and *y* vibrations as well as the tooth angle according to $n = x\sin(\phi) - y\cos(\phi)$.

For the simulation, the strategy is to divide the angle of the cut into a discrete number of steps. At each small time step, *dt*, the cutter angle is incremented by the corresponding small angle, $d\phi$. This approach enables convenient computation of the chip thickness for each simulation step because: 1) the possible teeth orientations are predefined; and 2) the surface created by the previous teeth at each angle may be stored. The cutter rotation $d\phi = \frac{360}{SR}$ (deg) depends on the selection of the number of steps per revolution, *SR*. The corresponding time step is $dt = \frac{60}{SR \cdot \Omega}$ (sec). A vector of angles is defined to represent the potential orientations of the teeth as the cutter is rotated through one revolution of the circular tool path, $\phi = [0, d\phi, 2\,d\phi, 3\,d\phi, \ldots, (SR-1)\,d\phi]$. The locations of the teeth within the cut are then defined by referencing entries in this vector.

In order to accommodate the helix angle for the tool's cutting edges, the tool may be sectioned into a number of axial slices. Each slice is treated as an individual straight tooth endmill, where the thickness of each slice is a small fraction, *db*, of the axial depth of cut, *b*. Each slice incorporates a distance delay $r\chi = db\tan(\gamma)$ relative to the prior slice (nearer the cutter free end), which becomes the angular delay between slices: $\chi = \frac{db\tan(\gamma)}{r} = \frac{2db\tan(\gamma)}{d}$ (rad) for the rotating endmill, where *d* is the endmill diameter and γ is the helix angle. In order to ensure that the angles for each axial slice match the predefined tooth angles, the delay angle between slices is $\chi = d\phi$. This places a constraint on the *db* value. By substituting $d\phi$ for χ and rearranging, the required slice width is $db = \frac{d \cdot d\phi}{2\tan(\gamma)}$.

Using the time-domain simulation approach, the forces and displacements may be calculated. These results are then once-per-revolution sampled to generate the bifurcation diagrams.

4 Results

In this study, the potential effects of retention knob design on the machine-spindle-holder-tool dynamics were evaluated using a simple geometry artifact and impact testing. For the three representative knob designs evaluated, no significant influence on the assembly frequency response was identified.

As noted, the semi-discretization method was applied to predict Hopf and period-2 bifurcation; see Fig. 3. These predictions were verified experimentally and were reported in (Govekar *et al.*). The up milling tests were completed using an 8 mm diameter endmill (mounted in a shrink fit tool holder) with one cutting edge, a 45 deg helix angle, and a 96 mm overhang. The radial depth of cut was 0.4 mm to provide highly interrupted cutting conditions. The aluminum workpiece and tool combination yielded a force model with a specific cutting force of 644 MPa and 69.7 deg force angle.

The long, slender tool exhibited a single dominant bending mode. The modal parameters for the *x* (feed) and *y* directions are provided in Table 1.

Table 1: Modal parameters obtained from impact testing.

Direction	Natural frequency (Hz)	Damping ratio (-)	Stiffness (N/m)
x	721	0.009	4.1×10^5
y	721	0.009	4.1×10^5

The stability diagram obtained from the semi-discretization method is plotted again in Fig. 5. However, lines are added that depict the spindle speeds that were used for the extended milling bifurcation diagrams. The modifier “extended” is used to emphasize that axial depths well beyond the predicted stability limit were used.

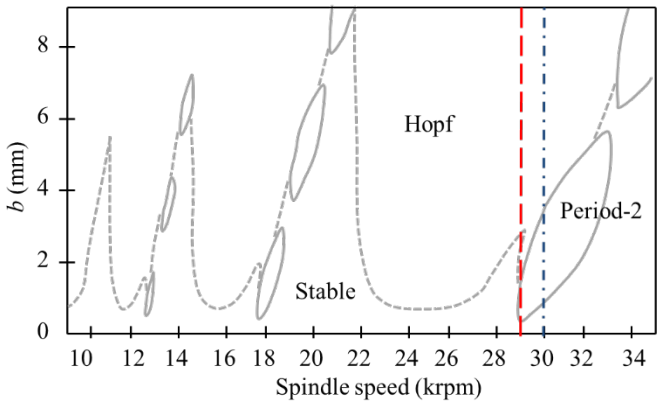

Figure 5. Stability lobe diagram with stable and unstable (Hopf and period-2) zones (Govekar *et al.*). Test speeds for the bifurcation diagrams are identified: (dashed line) 29000 rpm; (dash-dot line) 30000 rpm.

In Fig. 5 it is observed that the 29000 rpm (dashed) line predicts stable behavior up to an axial depth of 0.3 mm. Period-2 instability then occurs up to an axial depth of 2 mm. Stable performance is again predicted until 2.5 mm. Hopf instability then occurs for higher depths of cut.

The corresponding bifurcation diagram is presented in Fig. 6. The vertical axis represents the once-per-revolution sampled *x*-direction tool motions, while the horizontal axis is the axial depth of cut. The transition from stable to period-2 motion occurs at 0.26 mm; the period-2 instability persists with increasing amplitude until an axial depth of 2.1 mm. Stable operation is again obtained at 2.1 mm and is maintained until 2.4 mm. Hopf instability then occurs. The second stable zone validates the closed islands of stability depicted in Figs. 3 and 5. Regions of period-7 (3.38 mm to 3.54 mm) and period-5 (4.48 mm to 4.7 mm) instability are also observed. This behavior is not predicted by existing milling stability theory and, to the author's knowledge, has not been previously presented in the literature.

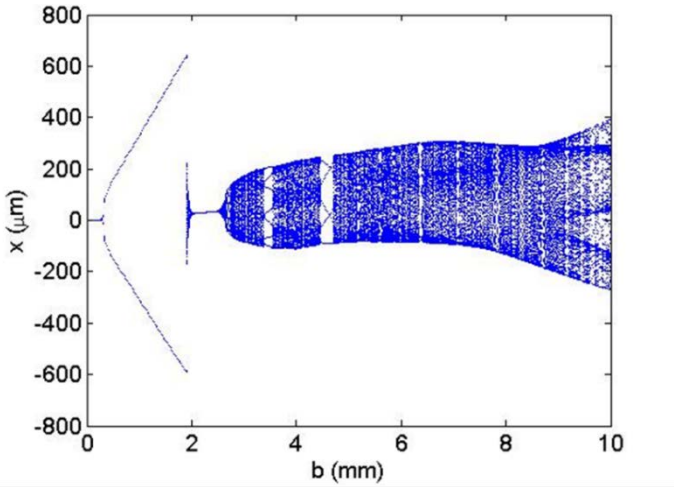

Figure 6. Extended milling bifurcation diagram (29000 rpm).

The corresponding bifurcation diagram is presented in Fig. 6. The vertical axis represents the once-per-revolution sampled *x*-direction tool motions, while the horizontal axis is the axial depth of cut. The transition from stable to period-2 motion occurs at 0.26 mm; the period-2 instability persists with increasing amplitude until an axial depth of 2.1 mm. Stable operation is again obtained at 2.1 mm and is maintained until 2.4 mm. Hopf instability then occurs. The second stable zone validates the closed islands of stability depicted in Figs. 3 and 5. Regions of period-7 (3.38 mm to 3.54 mm) and period-5 (4.48 mm to 4.7 mm) instability are also observed. This behavior is not predicted by existing milling stability theory and, to the author's knowledge, has not been previously presented in the literature.

A bifurcation diagram was also produced for 30000 rpm (dash-dot line in Fig. 5). In Fig. 7, a transition from stable to period-2 motion is seen at 0.68 mm. The period-2 behavior persists to an axial depth of b = 1.26 mm where combination period-2 and quasi-periodic motion occurs. This is exhibited by the two separate vertical spreads in points. At 1.88 mm, the motion changes to quasi-periodic only and a single, vertical distribution of once-per-revolution sampled points is seen.

The significance of the extended range bifurcation diagram is seen at an axial depth of 4.76 mm. A dramatic amplitude reduction is observed at this depth, even though the cut remains unstable. This reduced amplitude at a high axial depth could provide acceptable cutting conditions, while offering a high material removal rate. Additionally, period-7 instability is predicted in the range from b = 5.48 mm to 5.66 mm. As noted, milling stability theory does not predict this behavior. These results call for additional analysis and experiments to better understand the predicted behavior.

These results demonstrate that the extended milling bifurcation diagram is a powerful tool to enable a detailed view of unstable behavior and elicit an improved understanding of milling dynamics. It is expected that this new understanding will lead to new milling strategies that improve productivity.

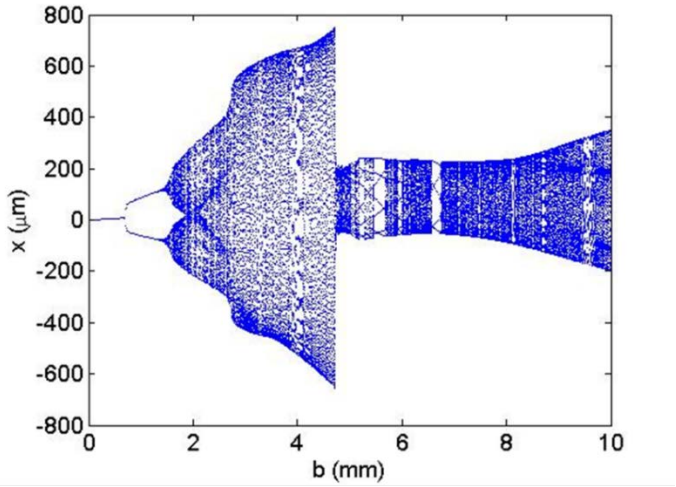

Figure 7. Extended milling bifurcation diagram (30000 rpm).

5 Discussion

The initial results presented here serve to motivate follow-on experiments and analyses. The period-*n* bifurcations and reduced vibration amplitude at high (unstable) axial depths of cut should be verified with cutting tests. The setup shown in Fig. 2 could again be implemented to measure and sample the tool motions during cutting. For the time-domain simulation, the circular tool path approximation could be extended to consider the actual cycloidal motion of the cutter teeth (Schmitz and Smith). This may offer new information since the phenomena investigated here are specific to low radial immersion milling.

6 Conclusions

This paper described the extended milling bifurcation diagram, which was constructed using time-domain simulation and once-per-revolution sampling. The diagram describes both stability behavior (such as Hopf and period-*n* bifurcations) and vibration amplitudes under stable and unstable conditions. New milling phenomena were predicted, including period-*n* bifurcations and reduced vibration amplitudes at high (unstable) axial depths of cut. It is expected that the insights gained through the extended milling bifurcation diagram will reveal new milling strategies that yield increased productivity and reduced costs for subtractive, discrete part manufacturing.

References

Altintas, Y. and Budak, E. (1995). Analytical prediction of stability lobes in milling. *Annals of the CIRP*, 44(1), 357-362.

Arnold, R. N. (1946). The mechanism of tool vibration in the cutting of steel, In: *Proceedings of the Institute of Mechanical Engineers*, 154.

Bukkapatnam, S., Lakhtakia, A., and Kumara, S. (1995). Analysis of senor signals shows turning on a lathe exhibits low-dimensional chaos. *Physics Review E*, 52, 2375-2387.

Campomanes, M. L. and Altintas, Y. (2003). An improved time domain simulation for dynamic milling at small radial immersions. *ASME Journal of Manufacturing Science and Engineering*, 125(3), 416-422.

Davies, M. A., Dutterer, B. S., Pratt, J. R., and Schaut, A. J. (1998). On the dynamics of high-speed milling with long, slender endmills. *Annals of the CIRP*, 47(1), 55-60.

Davies, M. A., Pratt, J. R., Dutterer, B. S., and Burns, T. J. (2000). The stability of low radial immersion milling. *Annals of the CIRP*, 49(1), 37-40.

Davies, M. A., Pratt, J. R., Dutterer, B. S., and Burns, T. J. (2002). Stability prediction for low radial immersion milling, *ASME Journal of Manufacturing Science and Engineering*, 124, 217-225.

Doi, S. and Kato, S. (1956). Chatter vibration of lathe tools. *Transactions of the ASME*, 78, 1127-1134.

Govekar, E., Gradišek, J., Kalveram, M., Insperger, T., Weinert, K., Stepan, G., and Grabec, I. (2005). On stability and dynamics of milling at small radial immersion. *Annals of the CIRP*, 54(1), 357-362.

Gradišek, J., Kalveram, M., Insperger, T., Weinert, K., Stépán, G., Govekar, E., and Grabec, I. (2005). On stability prediction for milling. *International Journal of Machine Tools and Manufacture*, 45(7-8), 769-781.

Hanna, N. H. and Tobias, S. A. (1974). A theory of nonlinear regenerative chatter. *ASME Journal of Engineering of Industry*, 96, 247-255.

Hohn, R. E., Shridar, R., and Long, G.W. (1968). A stability algorithm for a special case of the milling process, *ASME Journal of Engineering for Industry*, 90, 326-329.

Insperger, T., Munoa, J., Zatarain, M. A., and Peigné, G. (2006). Unstable islands in the stability chart of milling processes due to the helix angle, In: *CIRP 2nd International Conference on High Performance Cutting*, Vancouver, Canada, June, 12-13.

Insperger, T. and Stépán, G. (2004). Vibration frequencies in high-speed milling processes or A positive answer to Davies, Pratt, Dutterer, and Burns. *ASME Journal of Manufacturing Science and Engineering*, 126(3), 481-487.

Insperger, T., Stépán, G., Bayly, P. V., and Mann, B. P. (2003). Multiple chatter frequencies in milling processes. *Journal of Sound and Vibration*, 262, 333-345.

Mann, B. P., Bayly, P. V., Davies, M. A., and Halley, J. E. (2004). Limit cycles, bifurcations, and accuracy of the milling process. *Journal of Sound and Vibration* 2004; 277: 31-48.

Mann, B. P., Garg, N. K., Young, K. A, and Helvey, A. M. (2005). Milling bifurcations from structural asymmetry and nonlinear regeneration. *Nonlinear Dynamics*, 42(4), 319-337.

Mann, B. P., Insperger, T., Bayly, P. V., and Stépán, G. (2003). Stability of up-milling and down-milling, Part 1: Alternative analytical methods. *International Journal of Machine Tools and Manufacture*, 43(1), 25-34.

Mann, B. P., Insperger, T., Bayly, P. V., and Stépán, G. (2003). Stability of up-milling and down-milling, Part 2: Experimental verification. *International Journal of Machine Tools and Manufacture* 2003; 43(1): 35-40.

Merdol, S. D. and Altintas, Y. (2004). Multi frequency solution of chatter stability for low immersion milling. *ASME Journal of Manufacturing Science and Engineering*, 126, 459–466.

Merritt, H. E. (1965). Theory of self-excited machine-tool chatter. *ASME Journal of Engineering for Industry*, 87, 447-454.

Minis, I. and Berger, B. S. (1998). Modelling, analysis, and characterization of machining dynamics, In: *Dynamics and Chaos in Manufacturing Processes* (Ed. F.C. Moon), Wiley, 125-163.

Minis, I. and Yanusevsky, R. (1993). A new theoretical approach for prediction of chatter in milling. *ASME Journal of Engineering for Industry*, 115, 1-8.

Moon, F. C. (1994). Chaotic dynamics and fractals in material removal processes. In: *Nonlinearity and Chaos in Engineering Dynamics* (Ed. J. Thompson and S. Bishop), Wiley, 25-37.

Moon, F. C. and Johnson, M. (1998). Nonlinear dynamics and chaos in manufacturing processes, In: *Dynamics and Chaos in Manufacturing Processes* (Ed. F.C. Moon), Wiley, 3-32.

Moon, F. C. and Kalmár-Nagy, T. (2001). Nonlinear models for complex dynamics in cutting materials. *Philosophical Transactions of the Royal Society London A*, 359: 695-711.

Nayfey, A., Chin, C., and Pratt, J. (1998). Applications of perturbation methods to tool chatter dynamics. In: *Dynamics and Chaos in Manufacturing Processes* (Ed. F.C. Moon), Wiley, 193-213.

Patel, B. R., Mann, B. P., and Young, K. A. (2008). Uncharted islands of chatter instability in milling. *International Journal of Machine Tools and Manufacture*, 48(1), 124-134.

Schmitz, T. and Smith, K. S. (2009). *Machining Dynamics: Frequency Response to Improved Productivity*. New York: Springer.

Shridar, R., Hohn, R. E., and Long, G. W. (1968). A general formulation of the milling process equation. *ASME Journal of Engineering for Industry*, 90, 317-324.

Shridar, R., Hohn, R. E., and Long, G. W. (1968). A stability algorithm for the general milling process. *ASME Journal of Engineering for Industry*, 90, 330-334.

Smith, K. S. and Tlusty, J. (1991). An overview of modeling and simulation of the milling process. *ASME Journal of Engineering for Industry*, 113, 169-175.

Stépán, G. and Kalmár-Nagy, T. (1997). Nonlinear regenerative machine tool vibrations. In: *Proceedings of the 1997 ASME Design Engineering Technical conference on Vibration and Noise*. Sacramento, CA, DETC 97/VIB-4021, 1-11.

Stépán, G., Szalai, R., Mann, B. P., Bayly, P. V., Insperger, T., Gradisek, J., and Govekar, E. (2005). Nonlinear dynamics of high-speed milling – Analyses, numerics, and experiments. *Journal of Vibration and Acoustics*, 127, 197-203.

Tobias, S. A. (1965). *Machine Tool Vibration*. New York: Wiley.

Tobias, S. A. and Fishwick, W. (1958). The chatter of lathe tools under orthogonal cutting conditions. *Transactions of the ASME*, 80, 1079-1088.

Tlusty, J. (1985). Machine dynamics, In: *Handbook of High-speed Machining Technology* (Ed. R.I. King). New York: Chapman and Hall, 48-153.

Tlusty, J. (1986). Dynamics of high-speed milling, *ASME Journal of Engineering for Industry*, 108, 59-67.

Tlusty, J. and Ismail, F. (1981). Basic non-linearity in machining chatter. *Annals of the CIRP*, 30, 299-304.

Tlusty, J. and Ismail, F. (1983). Special aspects of chatter in milling. *ASME Journal of Vibration, Stress and Reliability in Design*, 105, 24-32.

Tlusty, J. and Polacek, M. (1963). The stability of machine tools against self-excited vibrations in machining. In: *Proceedings of the ASME International Research in Production Engineering Conference*, Pittsburgh, PA, 465-474.

Tlusty, J. and Polacek, M. (1968). Experience with analysing stability of machine tool against chatter. In: *Proceedings of the 9th MTDR Conference*, 521-570.

Zatarain, M., Muñoa, J., Peigné, G., and Insperger, T. (2006). Analysis of the influence of mill helix angle on chatter stability. *Annals of the CIRP*, 55(1), 365-368.

Zhao, M. X. and Balachandran, B. (2001). Dynamics and stability of milling process. *International Journal of Solids and Structures*, 38, 2233-2248.